· Article · Advances in Polar Science
doi: 10.13679/j.advps.2018.3.00205 September 2018 Vol. 29 No. 3: 205-214

Trends of summertime extreme temperatures in the Arctic

SUI Cuijuan[1*] & YU Lejiang[2,3]

[1] National Marine Environmental Forecasting Center, Beijing 100081, China;
[2] Polar Research Institute of China, Shanghai 200136, China;
[3] SOA Key Laboratory for Polar Science, Shanghai 200136, China

Received 23 April 2018; accepted 15 September 2018

Abstract Extreme temperature events can influence the natural environment and societal activities more so than mean temperature events. This study used daily data from 238 stations north of 60°N, obtained from the Global Summary of the Day dataset for the period 1979–2015, to investigate the trends of summertime extreme temperature. The results revealed most stations north of 60°N with trends of decrease in the number of cold days (nights) and increase in the number of warm days (nights). The regional average results showed trends of consistent decline (rise) of cold days and nights (warm days and nights) in Eurasia and Greenland. Similarly, the trends of the seasonal maximum and minimum values were most significant in these regions. In summer, of three indices considered (i.e., Arctic Oscillation, Arctic dipole, and El Niño–Southern Oscillation), the largest contributor to the trends of extreme temperature events was the Arctic dipole. Prevailing southerly winds in summer brought warm moist air across northern Eurasia and Greenland, conducive to increased numbers of warm days (nights) and decreased numbers of cold day (nights). Moreover, we defined extreme events using different thresholds and found the spatial distributions of the trends were similar.

Keywords **extreme temperature events, north of 60°N, trend analysis, abrupt change analysis, composite analysis**

Citation: Sui C J, Yu L J. Trends of summertime extreme temperatures in the Arctic. Adv Polar Sci, 2018, 29(3): 205-214, doi: 10.13679/j.advps.2018.3.00205

1 Introduction

Temperatures in the Arctic are increasing twice as fast as the global average, which is a phenomenon known as Arctic amplification (Overland et al., 2013; Stroeve et al., 2012; Serreze and Barry, 2011). In conjunction with this increase in mean temperature, large numbers of extreme events have occurred during the previous decade. It is obvious that the natural environment, society, economies, and human health are more vulnerable to extreme climatic events than to average climate conditions (Easterling et al., 2000), especially extreme temperature and weather (Yu et al., 2016).

Extreme temperature events are associated with climate warming. The process of climate warming complicates the relationship between the tropics and the poles. It accentuates the imbalance in the original heating, which increases atmospheric instability and leads to frequent extreme events. During the previous three winter seasons, extreme warming events have been observed over the sea ice in the central Arctic Ocean. Each warming event, which persisted for 1–3 d, was associated with temperatures close to or above 0℃. Typically, temperatures in the Arctic in winter are below −30℃ (Graham et al., 2017). However, our understanding of the regional trends of Arctic weather and climate extremes remains poor because of the lack of observational data. In fact, Arctic extreme temperature events are also of major societal relevance because they can

* Corresponding author, E-mail: suicj@nmefc.cn

have substantial influence on the ecological environment and produce considerable challenges in relation to infrastructure (Yu et al., 2017; Rennert et al., 2009). Hence, it is necessary to investigate the changes and variability of Arctic extreme temperature events.

Extreme temperature indices are defined in various ways and for further details of specific indices, the reader is referred to the CLIMDEX website (http://www.climdex.org/indices.html). Matthes et al. (2015) revealed the temporal evolution and variability of temperature in winter and summer during 1979–2013 using two indices: Cold Spells and Warm Spells. Sui et al. (2017) investigated the trends of Arctic air temperature extremes north of 60°N in winter based on cold days, cold nights, warm days, and warm nights. Thus, different extreme temperature indices can be selected depending on the requirements of a particular study.

There have been fewer studies of extreme temperature events north of 60°N in summer in comparison with winter (Graham et al., 2017; Sui et al., 2017; Cassano et al., 2016; Yu et al., 2016). In fact, summer temperatures can directly affect the extent of autumn sea ice, and the extent of sea ice is closely related to Arctic winter temperature. Investigation of the trend of summer extreme events could facilitate further understanding of the Arctic climate and provide a reference base for scientific activities and maritime cargo transport. Using station data, this study focused on the trends of extreme temperature north of 60°N during summer and their potential underlying causes. The remainder of the paper is organized as follows. Section 2 describes the data sources, definition of extreme events, and statistical methods adopted. The results of the trend analysis and possible reasons that could explain the elucidated trends are presented in Section 3. Finally, our conclusions are outlined in Section 4.

2 Data and methods

We used daily maximum and minimum temperature data from 238 stations north of 60°N, which were obtained from the Global Summary of the Day dataset that is processed and distributed by the National Climate Data Center (www.ncdc.noaa.gov/oa/mpp/freedata.html). These data were used to calculate various temperature indices for summer (June–August) during 1979–2015. Ultimately, eight temperature indices were selected, as described in Table 1. All the daily maximum temperature data for the summers during 1979–2015 were used to derive a distribution of daily maximum temperature. The 90th (95th) percentile of the distribution was used as the threshold for warm days, i.e., a daily maximum temperature in summer was considered a warm day when it exceeded the threshold. The 10th (5th) percentile of the distribution was used as the threshold for extreme cold events, i.e., it was considered a cold day when the daily maximum temperature in summer was less than the threshold. A similar process was applied to the daily minimum temperature to obtain distributions of warm and cold nights in summer. In addition, *TXx*, *TXn*, *TNx*, and *TNn* were defined as extreme seasonal values.

Table 1 Definitions of temperature indices used in this study (T_{max} and T_{min} are the daily maximum and minimum temperatures, respectively)

Variable	Indicator name	Definition
T_{max}	Warm days/d	No. of days with T_{max}> 90th (95th) percentile
	Cold days/d	No. of days with T_{max}< 10th (5th) percentile
	TXx/℃	Seasonal maximum value of daily maximum temperature
	TXn/℃	Seasonal minimum value of daily maximum temperature
T_{min}	Warm nights/d	No. of days with T_{min}> 90th (95th) percentile
	Cold nights/d	No. of days with T_{min}< 10th (5th) percentile
	TNx/℃	Seasonal maximum value of daily minimum temperature
	TNn/℃	Seasonal minimum value of daily minimum temperature

Monthly large-scale atmospheric circulation data with horizontal resolution of 0.75° × 0.75° obtained during 1979–2015 were extracted from the ERA-Interim reanalysis dataset, which is produced by the European Centre for Medium-Range Weather Forecasts (Dee et al., 2011; http://www.ecmwf.int/en/research/climate-reanalysis/era-interim). These data included sea level pressure, surface wind, downward longwave radiation, and 500-hPa geopotential. The oceanic dataset for the same period comprised Advanced Very High Resolution Radiometer data of sea surface temperature with horizontal resolution of 0.25° × 0.25°. The Arctic Oscillation (AO) and the Arctic dipole (DA) indices were defined as the standardized leading two modes of empirical orthogonal function analysis of monthly sea level pressure anomaly poleward of 70°N. The monthly El Niño–Southern Oscillation (ENSO) index is available from the following website: http://www.cpc.ncep.noaa.gov/data/indices/.

Trend analyses, the Mann–Kendall trend test (Kendall, 1955; Mann, 1945), and composite analysis were used to identify the interannual variability of summertime extreme temperature events and to explore the possible underlying reasons behind them. The Mann–Kendall statistics test has been used frequently to quantify the significance of trends in hydrometeorological time series and to examine abrupt change points. First, we constructed one sequence as Eq. (1) and m_i as a function, as in Eq. (2), where n is the number of total data points, and x_i and m_j are the data values in time series i and j ($i > j$), respectively.

$$d_k = \sum_{i=1}^{k} m_i \quad (2 \leqslant k \leqslant n) \tag{1}$$

$$mi = \begin{cases} +1 & \text{if } x_i > x_j \\ 0 & \text{if } x_i \leqslant x_j \end{cases} \quad k = 1, 2 \cdots i \tag{2}$$

The mean and variance of the Mann–Kendall statistic were calculated using Eqs. (3) and (4), respectively, and the standard normal test statistic UF_k was estimated using Eq. (5). Then, UF_k was used to form a line UF showing increasing or decreasing trends.

$$E(d_k) = k(k-1)/4 \tag{3}$$

$$\mathrm{Var}(d_k) = k(k-1)(2k+5)/72 \tag{4}$$

$$UF_k = \frac{d_k - E(d_k)}{\sqrt{\mathrm{var}(d_k)}} \tag{5}$$

The above process was repeated using the anti-sequence (x_n, x_{n-1}, $\cdots$, x_1)) and the order $UB_k = -UF_k$ to obtain line UB. The intersection of lines UF and UB in the significance level was taken as the abrupt change point.

All the linear trends were partitioned into linearly congruent and linearly independent (or residual) components with respect to the monthly AO, DA, and ENSO indices are as follows (Yu et al., 2013, 2011; Thompson and Wallace, 2000).

(a) Regress the number of extreme events of the time series onto the AO index.

(b) Multiply the resulting regression coefficients by the linear trend in the AO index.

(c) Trends that are linearly congruent with the monthly DA and ENSO indices are estimated using a similar method as for the AO index.

The residual trend can be defined as the trend obtained by subtracting the trends in the AO, DA, and ENSO indices from the total trend.

3 Results

3.1 Trends in extreme temperature indices north of 60°N

The spatial distribution of extreme temperature events in summer north of 60°N showed that the most significant trend of decrease in the number of cold days was more than −3 d·decade^{-1} in Greenland, Alaska, and the Nordic regions (Figure 1a), while the trend of decrease at most stations was

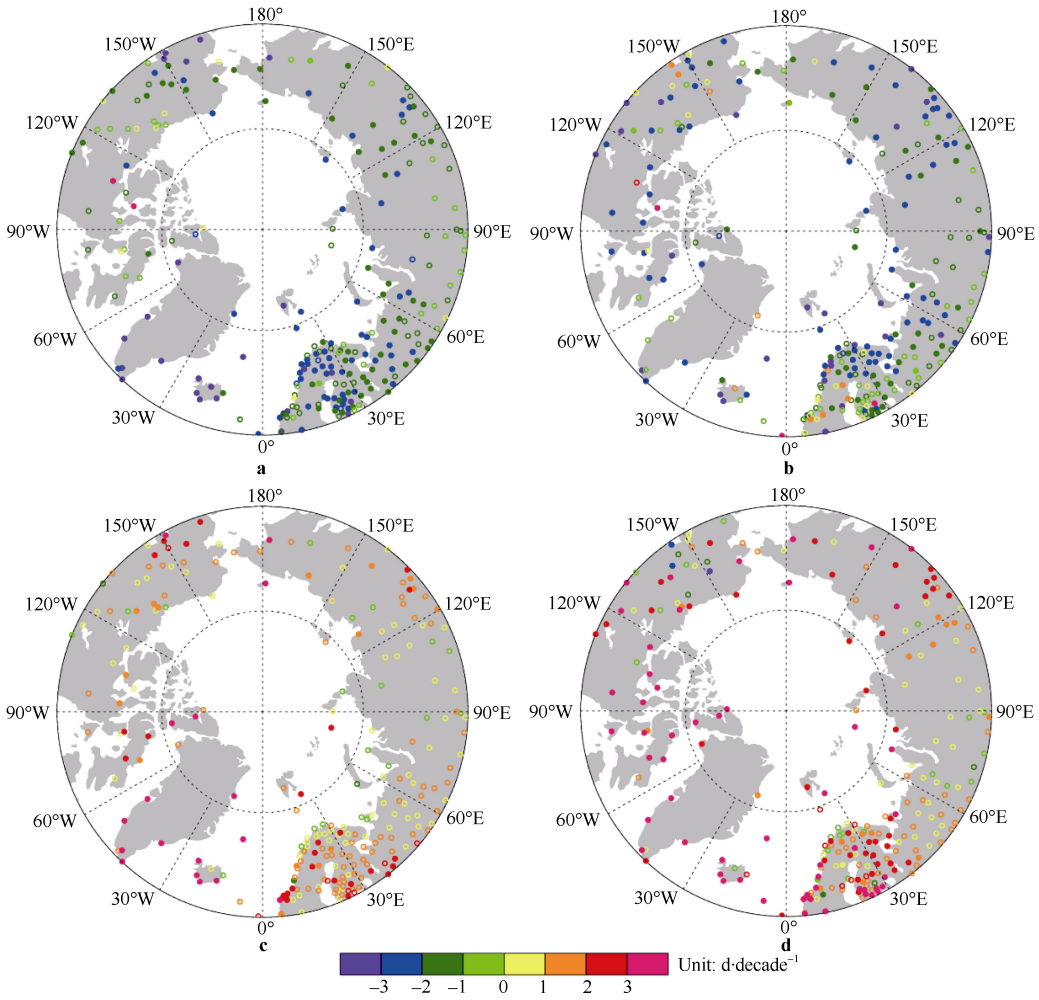

Figure 1 Trends of extreme temperature events in the Arctic in summer during 1979–2015: **a**, cold days; **b**, cold nights; **c**, warm days and **d**, warm nights, using the 10th and 90th percentiles to define extreme events. Stations with statistically significant results at the 95% confidence level are shown as solid circles.

between −3 and −2 d·decade^{-1}. However, there was a trend of increase in the number of cold days at two stations in Canada (3 d·decade^{-1}) and at one station in Norway (0–1 d·decade^{-1}). Stations with a trend of decrease in the number of cold nights of more than −3 d·decade^{-1} were scattered throughout the Arctic (Figure 1b), while most other stations showed a trend of decrease of between −3 and −2 d·decade^{-1}. A trend of increase was found at some stations in northwestern Eurasia, Alaska (1–2 d·decade^{-1}), and Canada (3 d·decade^{-1}), and the trend of increase in the number of cold nights was larger than in the number of cold days. The domain in which the trend in the number of warm days increased most significantly was Greenland (>3 d·decade^{-1}), while the trend of increase in northwestern Eurasia and Alaska was 2–3 d·decade^{-1}. The trend at most other stations was found positive but not statistically significant (Figure 1c). The stations with a significant trend of increase (up to 3 d·decade^{-1}) in the number of warm nights were in Greenland, Canada, and eastern Russia, while the trend at stations in mid-Eurasia was not statistically significant. Incidentally, there was a trend of decrease in the number of warm nights at certain stations in Alaska (Figure 1d).

In addition, we also studied the trends of cold and warm events using the 5th and 95th percentile thresholds (figure not displayed) and we found the spatial distribution of the patterns of trends similar to Figure 1. The number of stations with significant changes using the 10th and 90th (5th and 95th) percentile thresholds was 145 (135) for cold days, 146 (148) for cold nights, 62 (60) for warm days, and 117 (106) for warm nights. However, the magnitude of the trends of the extreme events decreased. For example, in Greenland, the trend of decrease in the number of cold days using the 10th (5th) percentile threshold was −2 (−1) d·decade^{-1} and the trend of increase in the number of warm days using the 90th (95th) percentile threshold was >3 (2–3) d·decade^{-1}.

We also studied the trend of the seasonal maximum (minimum) value using the daily maximum (minimum) temperature. It was found that the temperature at some stations exhibited significant warming (Figure 2) with

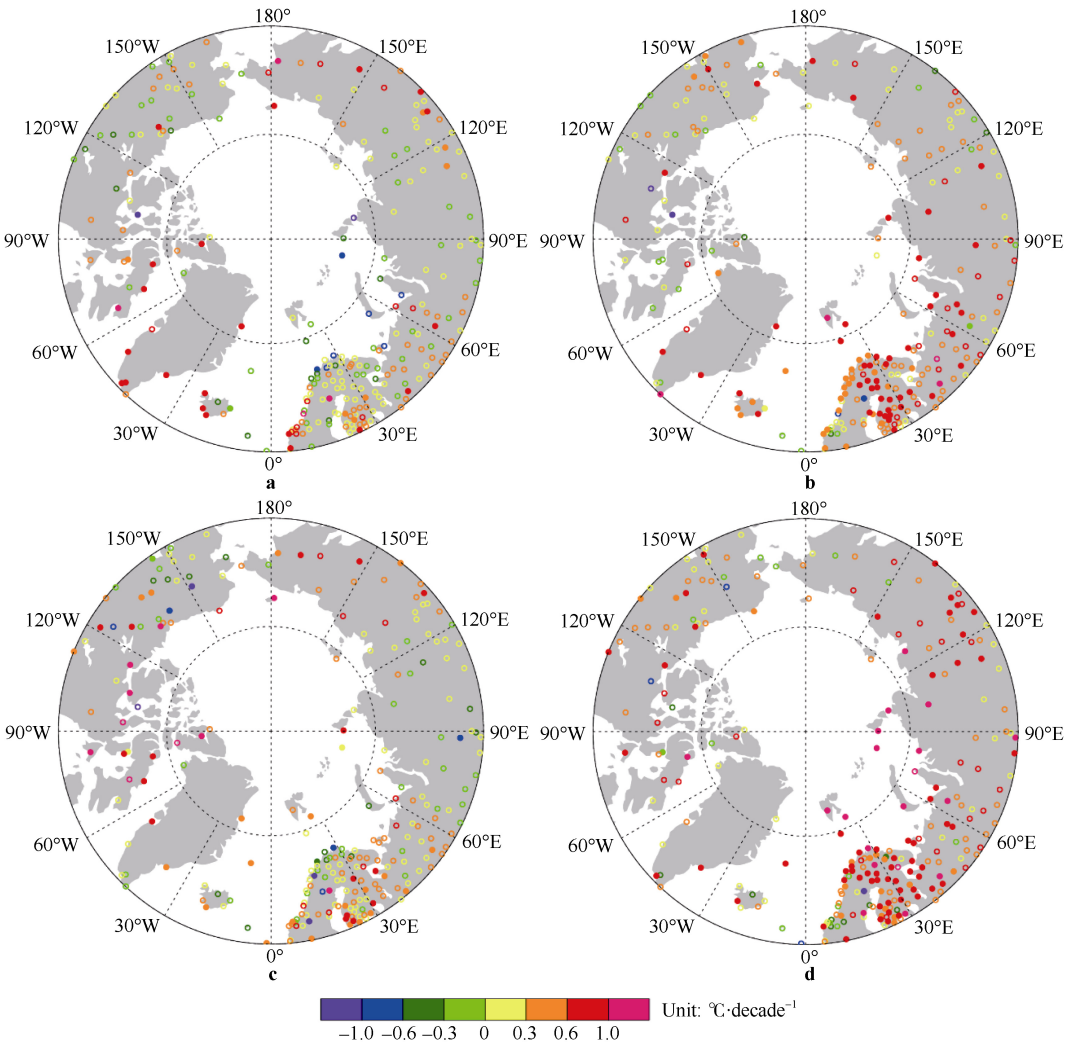

Figure 2 Trends of extreme temperature events in the Arctic in summer during 1979–2015: **a**, *TXx*; **b**, *TXn*; **c**, *TNx* and **d**, *TNn*. Stations with statistically significant results at the 95% confidence level are shown as solid circles.

magnitude of 0.3–1.0℃·decade^{-1}. However, some stations in Canada and Norway exhibited a decrease in maximum (minimum) temperature, similar to that shown in Figure 1.

Using the 90th percentile threshold, the trend in the numbers of cold days and nights (warm days and nights) decreased (increased) at most stations north of 60°N, with the exception of some stations in Canada and Norway. In comparison, using the 95th percentile threshold, the spatial patterns of the trend in extreme temperature events were similar to those of the 90th percentile threshold but their magnitudes were smaller. Among the four temperature indices, cold nights exhibited the most significant trend at the largest number of stations, followed by cold days. Warm nights exhibited the most significant trend at the smallest number of stations, which were located primarily in mid-Eurasia.

Kodra et al. (2014) noted that a 'Shifted Mean' and 'Increased Variability' can lead to intensifications of extremely cold and warm events in both tails of the distribution. Figure 3 reveals a significant trend of increase in the mean summertime maximum and minimum temperatures in northern Europe, Greenland, and some islands in the northern Atlantic Ocean, which would have favored increasing (decreasing) occurrence of warm (cold) days and nights in these regions. However, the trend of the variance of the summertime maximum and minimum temperatures was found not statistically significant (figure not shown). Thus, a significant trend of increase in the mean favors increasing (decreasing) occurrence of warm (cold) days and nights north of 60°N during summer.

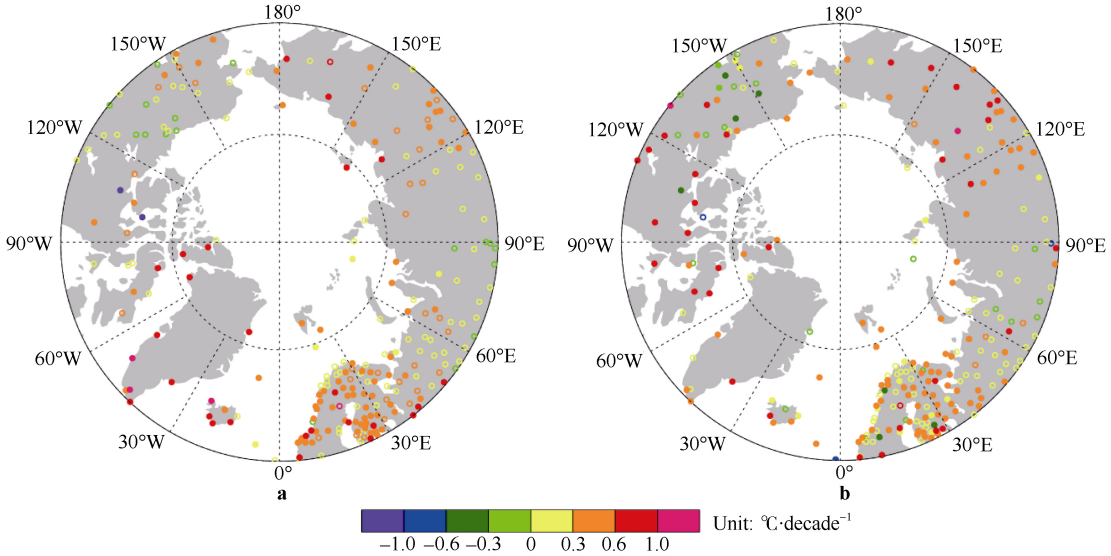

Figure 3 Trends of summertime means of T_{max} (**a**) and T_{min} (**b**) during 1979–2015. Stations with statistically significant results at the 95% confidence level are shown as solid circles.

To examine the physical linkage, we focused on the connection between the trends in the extreme temperature indices and the summertime atmospheric circulation, including sea level pressure, 10-m wind, and downward longwave radiation. Figure 4 shows that sea level pressure has been rising over northeastern Canada and Greenland and that the surface winds have become more anticyclonic. These findings are consistent with the results of previous studies (Ding et al., 2017; Serreze et al., 2016). The southerly direction of the wind anomaly in mid- and northeastern Eurasia was caused by anticyclonic anomalies over the Bering Strait and cyclonic anomalies over the Kara Sea. The prevailing southerly winds brought warm moist air in summer, which increased levels of humidity and downward longwave radiation (Figure 4c), conducive to increased numbers of warm days (nights) and decreased numbers of cold day (nights) in northeastern Eurasia and Greenland. Meanwhile, the trend of seasonal maximum (minimum) temperature in this region was mostly warming.

We examined the contributions of the AO, DA, and ENSO indices to the trends of cold days, cold nights, warm days, and warm nights (Figure 5). The largest contribution was from the DA index, followed by the AO index. The ENSO index was found to make the smallest contribution (magnitude: <0.5 d·decade^{-1}) to the trends of cold days, cold nights, warm days, and warm nights. The DA produced a negative trend in the number of cold days at most stations and a similar effect for the number of cold nights, with the exception of some stations in North Europe. The DA also resulted in negative (positive) trends in the numbers of warm days and nights in northern North Europe and central Russia (southern North Europe, northern Canada, and Greenland). The positive (negative) trends of warm (cold) days and nights in northeastern Canada and Greenland were found related to the AO index.

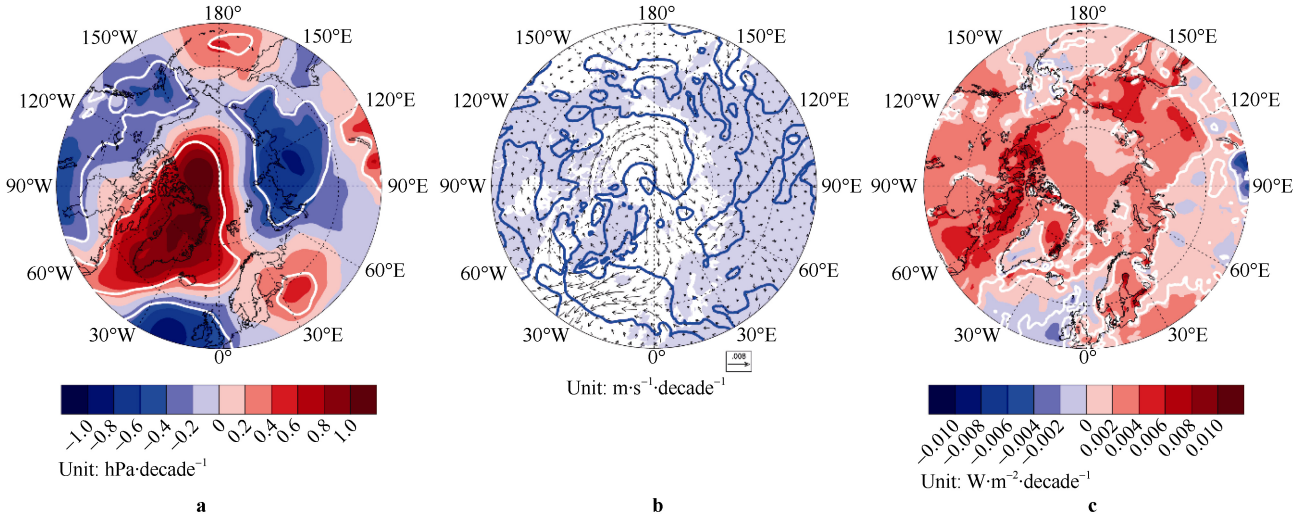

Figure 4 Trends of summertime sea level pressure (**a**), surface wind (**b**), and downward longwave radiation (**c**) during 1979–2015. Stations with statistically significant results at the 95% confidence level are shown as solid lines.

3.2 Trends in extreme temperature indices in different regions

The domain-averaged climate extremes were analyzed by calculating the average of the indices in five geographic regions: (1) northwestern Eurasia (including northern Europe, northern Russia west of the Ural Mountains, and the islands between 10°W and 60°E); (2) northeastern Eurasia (including northern Asia east of the Ural Mountains between 60°E and 165°W); (3) Alaska (between 165°W and 140°W); (4) Canada (including continental Canada and the islands between 140°W and 90°W), and (5) Greenland between 90°W and 10°W (Figure 6).

Table 2 shows the coefficients of the linear trend of eight indices in the five regions. The trends in the numbers of cold days and cold nights (warm days and warm nights) in Eurasia and Greenland showed consistent decline (rise), irrespective of whether the extreme index was calculated using the 5% (95%) or 10% (90%) thresholds. However, the trends of cold nights and warm nights (cold days and warm days) did not pass the significance test in Alaska (Canada). Similarly, the trend of the seasonal maximum and minimum values calculated using the daily maximum and minimum values were greatest in northwestern and northeastern parts of Eurasia and in Greenland. Only the trend of *TXn* in Alaska and of *TNx* in Canada increased significantly. In addition, the trend did not change in response to the change of threshold. These results verify the findings of the spatial distribution discussed in section 3.1.

We used the Mann–Kendall test to determine the abrupt changes in the trends of cold days, cold nights, warm days, and warm nights and the results are summarized in Table 3. The abrupt change point in most regions occurred in the mid-1990s. Therefore, we considered the fields of surface wind, 500-hPa geopotential, and sea surface temperature before and after 1995 (Figure 7).

Similar to Figure 4, the surface winds in Greenland were found more anticyclonic after 1995 because of a regional increase in sea level pressure (Figures 7b and 7d). The direction of the 10-m wind anomaly in Eurasia was southerly because of anticyclonic anomalies over the Bering Strait and cyclonic anomalies over the Kara Sea. The prevailing southerly winds brought warm moist air in summer across Eurasia and Greenland, conducive to increased numbers of warm days (nights) and decreased numbers of cold day (nights). These results, which are consistent with the findings of previous research (Wu et al., 2012), indicate that an anomalous cyclone that prevailed over the Arctic Ocean before 1997 was replaced by an anomalous anticyclone. Furthermore, the sea surface temperature was found to have increased across most of the North Atlantic, North Pacific, and Arctic oceans (Figure 7e), which would have increased the mean temperature and, subsequently, increased the number of warm days (nights) in the surrounding continental regions.

4 Conclusions

The impact of extreme temperature events is much greater than associated with average temperature events. Because of the sparse population and lack of data availability in the Arctic region, the study of extreme temperature events north of 60°N is lacking in comparison with regions further equatorward. Given the recent rapid melting of Arctic sea ice, the opening of an Arctic Passage is a realistic possibility and, consequently, there is urgent need for research of extreme temperature events in summer in the Arctic region. This study used daily maximum and minimum temperatures north of 60°N for the period 1979–2015, which were obtained from the Global Summary

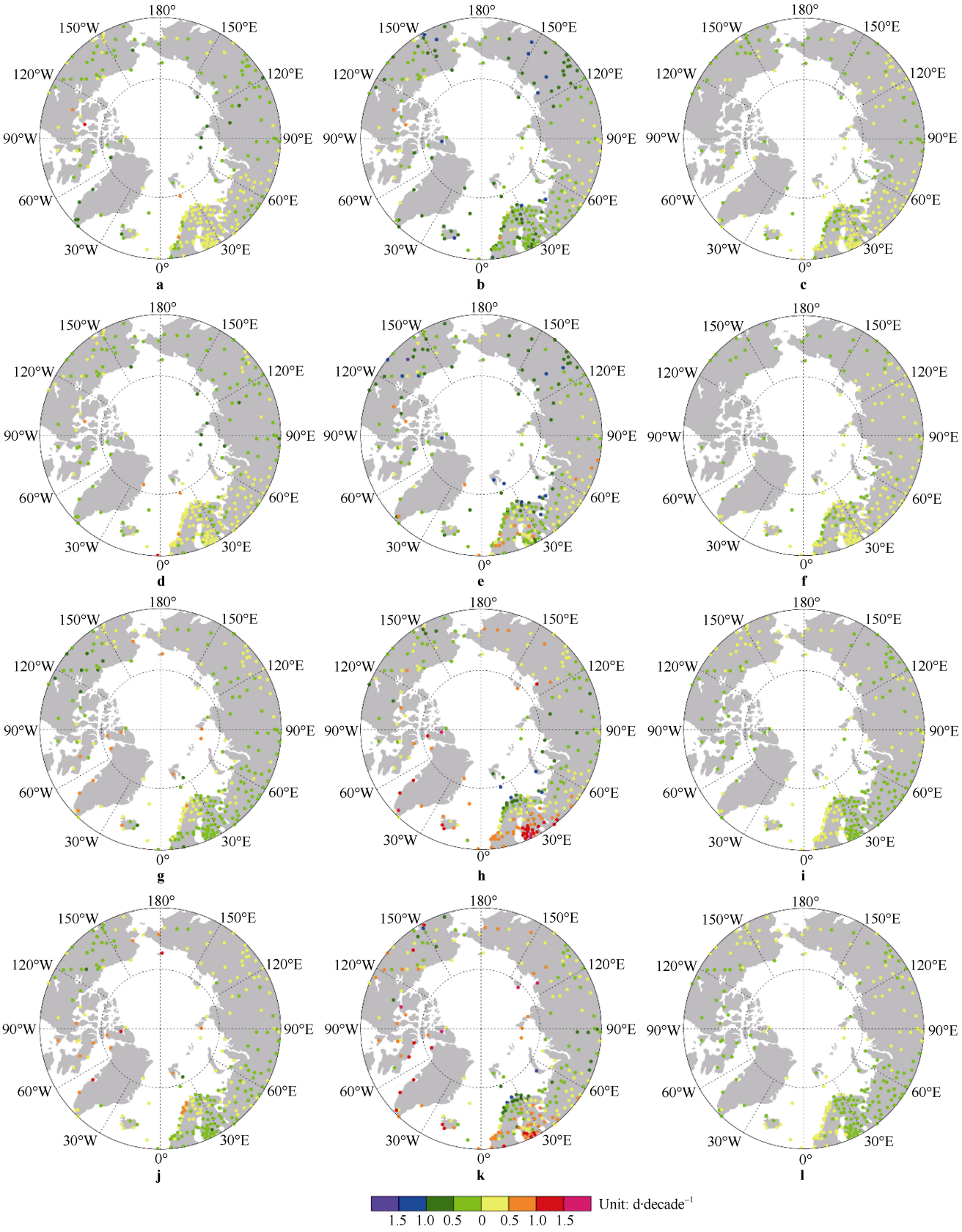

Figure 5 Trends of cold days, cold nights, warm days, and warm nights explained by the AO (**a–d**), DA (**e–h**), and ENSO indices (**i–l**).

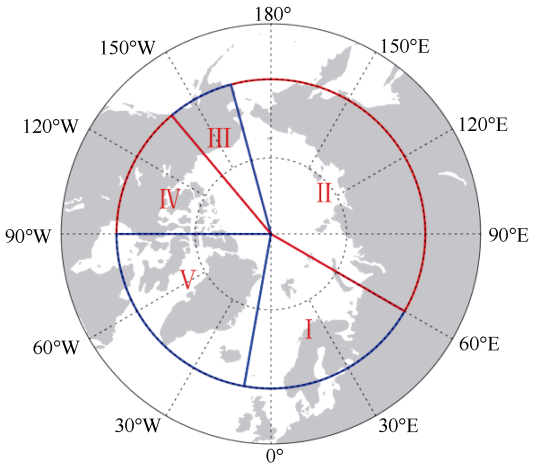

Figure 6 Schematic of the different regions investigated in this study: (I) northwestern Eurasia, (II) northeastern Eurasia, (III) Alaska, (IV) Canada, and (V) Greenland.

of the Day dataset. The following conclusions were derived through analysis of the summertime trends of eight temperature indices.

(a) The trend of cold days (nights) was decreased and that of warm days (nights) was increased north of 60°N in summer. The most significant trends of increase in cold days, warm days, cold nights, and warm nights were >3 d·decade^{-1} in Greenland, Alaska, and the Nordic regions, while the trends at other stations were between 1 and 3 d·decade^{-1}. The trend of the seasonal maximum (minimum) value of the daily maximum (minimum) temperature at those stations with significant change was warming with magnitude of 0.3–1.0℃·decade^{-1}; however, the trend at certain individual stations was the reverse. The trend in the numbers of cold days and cold nights (warm days and warm nights) in Eurasia (northwest and northeast) and Greenland displayed consistent decline (rise). Similarly, the trend of the seasonal maximum and minimum values was most obvious in the same regions.

Table 2 Trends in extreme temperature events in different regions (asterisks indicate statistical significance above the 95% confidence level, blue denotes negative trend, and red denotes positive trend)

Indicator	Thresholds (percentile)	Northwestern Eurasia	Northeastern Eurasia	Alaska	Canada	Greenland
Cold day/(d·decade^{-1})	10th	−1.9*	−1.4*	−2.3*	−0.1	−2.9*
	5th	−1.3*	−0.9*	−1.4*	0.1	−1.7*
Cold night/(d·decade^{-1})	10th	−1.3*	−1.8*	−0.8	−1.7*	−1.7*
	5th	−1.0*	−1.2*	−0.5	−0.8*	−1.0*
Warm day/(d·decade^{-1})	90th	1.3*	0.9*	0.18*	0.7	2.8*
	95th	0.9*	0.6*	1.2*	0.4	1.6*
Warm night/(d·decade^{-1})	90th	1.8*	1.4*	−0.1	2.3*	3.3*
	95th	1.2*	0.8*	0.2	1.3*	1.9*
TXx/(℃·decade^{-1})	---	0.18	0.20*	0.15	−0.05	0.56*
TXn/(℃·decade^{-1})	---	0.56*	0.48*	0.39*	−0.042	0.43*
TNx/(℃·decade^{-1})	---	0.23*	0.21*	−0.09	0.33*	0.46*
TNn/(℃·decade^{-1})	---	0.53*	0.64*	0.23	0.34	0.33*

Table 3 Abrupt change points in extreme temperature events in different regions

Indicator	Northwestern Eurasia	Northeastern Eurasia	Alaska	Canada	Greenland
Cold day	1994	---	1988	---	1994
Cold night	1988	1997	---	1993	1994
Warm day	1998	---	1986	1988	1996
Warm night	1997	1992	---	1996	1997

(b) The observed trends in extreme temperature events resulted from an abrupt change in 1994. After 1994, positive sea level pressure anomalies over northeastern Canada and Greenland induced prevailing southerly winds, conducive to increased numbers of warm days (nights) and decreased numbers of cold day (nights) in northern Eurasia and Greenland. Conversely, the opposite case was true prior to 1994. We also examined the contributions of the AO,

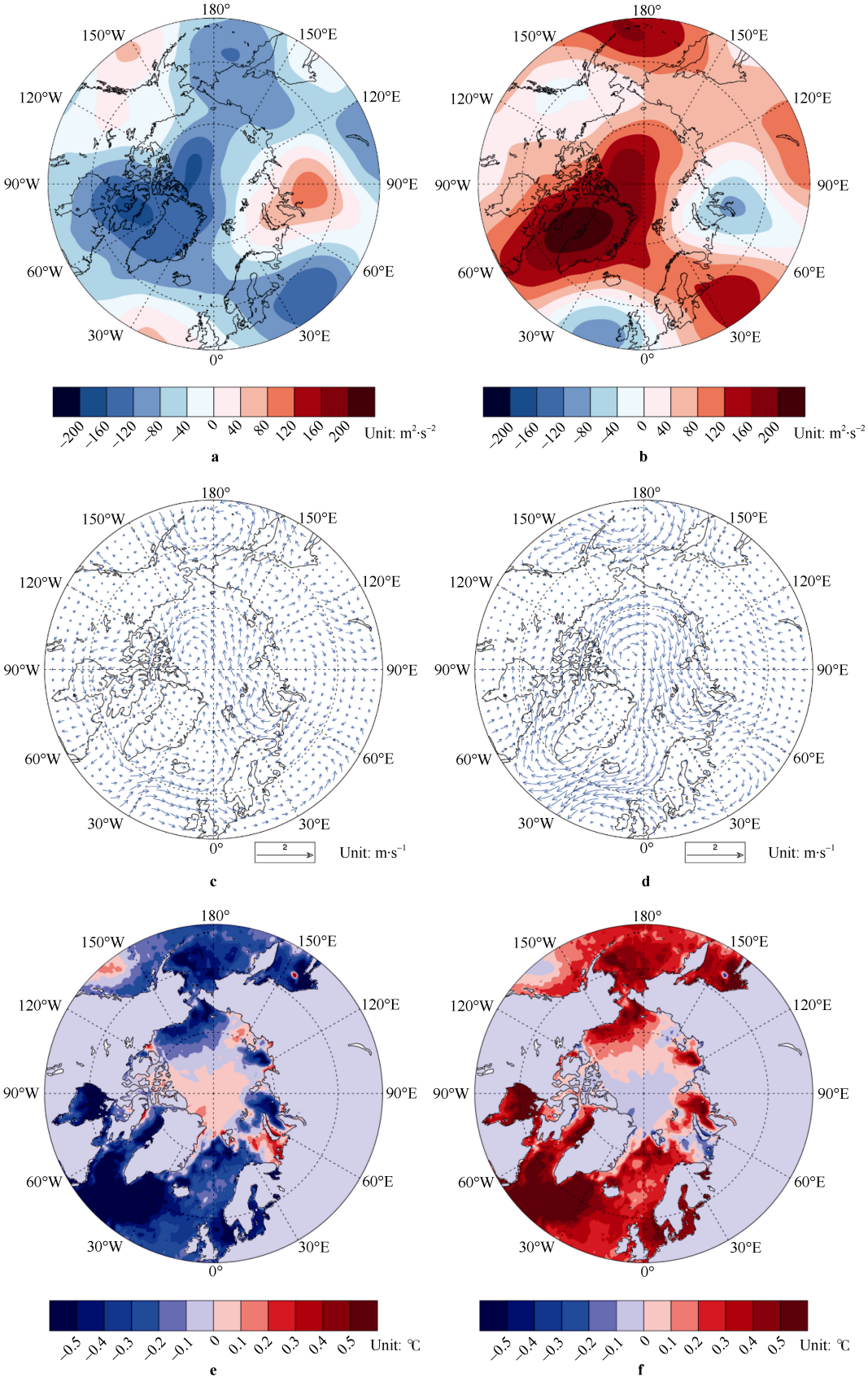

Figure 7 Composites of 500-hPa geopotential anomalies during 1979–1994 and 1994–2015 (**a**, **b**), respectively; 10-m wind anomalies during 1979–1994 and 1994–2015 (**c**, **d**), respectively; and SST anomalies during 1979–1994 and 1995–2015 (**e**, **f**), respectively.

DA, and ENSO indices. It was found that the largest contribution was from the DA index, followed by the AO index. In addition, a significant increasing trend was found in the mean summertime maximum and minimum temperatures in northern Europe, Greenland, and some islands in the northern Atlantic Ocean, which would have favored an increasing (decreasing) occurrence of warm (cold) days and nights in these regions. Meanwhile, the trend of the seasonal maximum (minimum) temperature in this region was mostly warming.

(c) For the 90th and 95th percentile thresholds, the spatial patterns of the trends in extreme temperature events were similar, although the magnitudes of the trends were somewhat different. Among the four temperature indices, cold nights had the most significant trend and warm nights had the smallest trend.

It was noticed that some stations, distributed mainly in Alaska, Canada, and Northern Europe, exhibited trends opposite to those of the extreme events, the underlying reasons for which we intend to analyze in subsequent research. Having elucidated the general trends of summertime air temperature extremes in regions north of 60°N, our future work will consider other variables such as extreme precipitation and wind.

Acknowledgments This work was supported by National Key R&D Program of China (Grant no. 2017YFE0111700) and Beijing Municipal Natural Science Foundation (Grant no. 8182023). We would like to thank the anonymous reviewers for their comments to improve this paper.

References

Cassano J J, Cassano E N, Seefeldt M W, et al. 2016. Synoptic conditions during wintertime temperature extremes in Alaska. J Geophys Res-Atmos, 121(7): 3241-3262.

Dee D P, Uppala S M, Simmons A J, et al. 2011. The ERA-Interim reanalysis: Configuration and performance of the data assimilation system. Q J R Meteorol Soc, 137(656): 553-597.

Ding Q, Schweiger A, L'Heureux M, et al. 2017. Influence of high-latitude atmospheric circulation changes on summertime Arctic sea ice. Nat Clim Change, 7(4): 289.

Easterling D R, Meehl G A, Parmesan C, et al. 2000. Climate extremes: observations, modeling, and impacts. Science, 289(5487): 2068-2074.

Graham R M, Cohen L, Petty A A, et al. 2017. Increasing frequency and duration of Arctic winter warming events. Geophys Res Lett, 44(13): 6974-6983, doi: 10.1002/2017GL073395.

Mann H B. 1945. Nonparametric tests againt trend. Econometrica, 13: 245-259.

Matthes H, Rinke A, Dethloff K. 2015. Recent changes in Arctic temperature extremes: warm and cold spells during winter and summer. Environ Res Lett, 10(11): 114020.

Kendall M G. 1955. Rank correlation methods. London: Griffin.

Kodra E, Ganguly A R. 2014. Asymmetry of projected increases in extreme temperature distributions. Sci Rep-UK, 4: 5884.

Overland J E, Wang M, Walsh J E, et al. 2013. Future Arctic climate changes: adaptation and mitigation time scales. Earths Future, 2(2): 68-74.

Rennert K J, Roe G, Putkonen J, et al. 2009. Soil thermal and ecological impacts of rain on snow events in the circumpolar Arctic. J Climate, 22(9): 2302-2315.

Serreze M C, Barry R G. 2011. Processes and impacts of Arctic amplification: a research synthesis. Global Planet Change, 77(1-2): 85-96.

Serreze M C, Stroeve J, Barrett A P, et al. 2016. Summer atmospheric circulation anomalies over the Arctic Ocean and their influences on September sea ice extent: A cautionary tale. J Geophys Res Atmos, 121(19): 463-485, doi: 10.1002/ 2016JD025161.

Sui C, Zhang Z, Yu L, et al. 2017. Investigation of Arctic air temperature extremes at north of 60°N in winter. Acta Oceanol Sin, 36(11): 51-60.

Stroeve J C, Serreze M C, Holland M M, et al. 2012. The Arctic's rapidly shrinking sea ice cover: a research synthesis. Climatic Change, 110(3-4): 1005-1027.

Thompson D W J, Wallace J M. 2000. Annular modes in the extratropical circulation. Part I: Month-to-month variability. J Climate, 13(5): 1000-1016.

Yu L, Zhang Z, Zhou M, et al. 2011. Interpretation of recent trends in Antarctic sea ice concentration. J Appl Remote Sens, 5(1): 053557.

Yu L, Zhang Z, Zhou M, et al. 2013. Trends in latent and sensible heat fluxes over the oceans surrounding the Arctic Ocean. J Appl Remote Sens, 7(1): 073531.

Yu L, Zhong S, Pei L, et al. 2016. Contribution of large-scale circulation anomalies to changes in extreme precipitation frequency in the United States. Environ Res Lett, 11(4): 044003.

Yu L, Sui C, Lenschow D H, et al. 2017. The relationship between wintertime extreme temperature events north of 60°N and large-scale atmospheric circulations. Int J Climatol, 37(S1): 597-611, doi: 10.1002/joc.5024.

Wu B, Overland J E, D'Arrigo R. 2012. Anomalous Arctic surface wind patterns and their impacts on September sea ice minima and trend. Tellus A, 64(1): 18590.